This is corrected version of manuscript with changes made according to the Reviewers' comments and submitted to ChemElectroChem. The final version is available here: **https://onlinelibrary.wiley.com/doi/abs/10.1002/celc.201900394**

Bismuth oxysulfide photoelectrodes with giant incident photon-to-current conversion efficiency: chemical stability in aqueous solutions

Evgeny A. Bondarenko[a], Eugene A. Streltsov*[a], Alexander V. Mazanik[a], Anatoly I. Kulak[b]

Abstract: Bismuth oxysulfide (BOS) films demonstrate giant incident photon-to-current conversion efficiency (IPCE >> 100%) under cathodic polarization. Their photoelectrochemical behavior and corrosion stability in aqueous solutions containing different redox systems ($[Fe(CN)_6]^{3-}$ /$[Fe(CN)_6]^{4-}$, Fe^{3+}/Fe^{2+}, I_2/I^-, S_n^{2-}/S^{2-}) has been investigated. We established that the chemical stability of the BOS is controlled mainly by three factors: (i) potentials of cathodic and anodic destruction of the BOS (Bi^{3+} reduction and S^{2-} oxidation), (ii) protolytic reactions leading to the dissolution of the semiconductor in acidic solutions at pH < 3, (iii) presence in solutions of anions, capable to participate in ion exchange reactions with the semiconductor forming poorly soluble compounds ($K[BiFe(CN)_6]\cdot 3H_2O$, BiOI and Bi_2S_3). The enrichment of the BOS surface with sulfur atoms (formation of S-terminated surface) gives rise to the substantial increase in the electrocatalytic activity of $[Fe(CN)_6]^{3-}$ cathodic reduction, which is accompanied by up to order increase of IPCE.

Introduction

Nowadays, there are a number of known bismuth oxysulfide compounds: Bi_2O_2S [1–3], Bi_2OS_2 [4], $Bi_3O_2S_3$ [5,6], $Bi_4O_4S_3$ [4,7-9], $Bi_9O_{7.5}S_6$ [10], $Bi_{10}O_6S_9$ [11]. These materials have a layered structure and are characterized by the pronounced anisotropy of electronic properties [1–17]. $Bi_3O_2S_3$ and $Bi_4O_4S_3$ are of great interest for superconductive materials design [9,14–16]. Bi_2O_2S, Bi_2OS_2, $Bi_9O_{7.5}S_6$ and $Bi_{10}O_6S_9$ with relatively low band gap energy (0.99 – 1.38 eV) are the promising compounds for photosensing and solar energy conversion [2,3,10,11].

Recently, our group has reported that the bismuth oxysulfide films prepared by the chemical bath deposition (CBD) generate the photocurrent under cathodic polarization and visible light illumination in a contact with aqueous solutions demonstrating incident photon-to-current conversion efficiency (IPCE) up to 2500% [11]. Characterization of the BOS films using scanning electron microscopy (SEM) revealed their layered structure. The BOS material is formed by the platelet crystallites with a thickness of several tens of nanometers and a length of a micrometer range. According to X-ray photoelectron spectroscopy, the BOS films contain bismuth and sulfur atoms in the oxidation states +3 and –2, respectively. The giant IPCE effect is observed for the BOS films with a wide Bi/S atomic ratio: from 1.1 to 2.6 [12].

The giant IPCE is determined by a decrease in a semiconductor film resistivity under illumination. It provides the possibility for charge carriers from external circuit to participate in the photoreduction process [11]. The abnormally high IPCE values are observed for cathodic processes in aqueous solutions which contain such acceptors of photoelectrons as $[Fe(CN)_6]^{3-}$, I_2, H_2O_2 and quinone. The giant IPCE appears starting from a certain minimum oxidizer concentration ($c > 10^{-3}$ M for $[Fe(CN)_6]^{3-}$) and reduces non-linearly with the increase of illumination intensity [11].

[a] E. A. Bondarenko, Prof. E. A. Streltsov, Dr. A. V. Mazanik
Belarusian State University
Nezavisimosti Av. 4, Minsk 220030, Belarus
E-mail: streltEA@bsu.by
[b] Prof. A. I. Kulak
Institute of General and Inorganic Chemistry
National Academy of Sciences of Belarus
Minsk 220072, Belarus

The chemically deposited BOS films are characterized by a very low lifetime of non-equilibrium charge carriers. These values are in the range of a few tens of picoseconds depending on the film thickness, and the charge carriers diffusion coefficient is below 1 $cm^2 \cdot s^{-1}$ [12]. It leads to a negligible contribution of diffusion in a charge transfer across the films evidencing that this process is determined mainly by drift. The main condition for the giant IPCE effect observation is the photogeneration of charge carriers over the entire film thickness [12]. Therefore, the increase of the BOS film thickness at a fixed wavelength of monochromatic light, as well as the shortening of wavelength at a fixed thickness result in a reduction of giant IPCE [12].

The giant IPCE effect is manifested in aqueous solutions containing various redox systems. For practical use of the giant IPCE effect, it is necessary to have information about the corrosion and photocorrosion stability of BOS films. The weak corrosion stability of many semiconductor electrodes is the key problem that restricts the perspectives for their use in photoelectrochemical converters of solar energy, chemotrones, supercapacitors and other devices. Along with the processes of photoelectrochemical corrosion in a contact with the electrolyte, surface chemical reactions of semiconductor with electrolyte components can occur. It results in formation of additional products on the surface. Depending on the amount of the precipitated products, their electrophysical and electrochemical properties, such coating can act as either blocking (barrier) layer or an electrocatalyst.

In this work we aim to determine corrosion and photocorrosion stability of BOS electrodes in aqueous solutions containing $[Fe(CN)_6]^{3-}/[Fe(CN)_6]^{4-}$, Fe^{3+}/Fe^{2+}, I_2/I^-, S_n^{2-}/S^{2-} redox-systems and to reveal the influence of BOS surface enrichment by sulfur atoms (S-terminated surface) on the IPCE value.

Results and Discussion

Giant IPCE effect on BOS electrodes in $[Fe(CN)_6]^{3-}$/ $[Fe(CN)_6]^{4-}$ containing solutions

The giant IPCE effect is observed under cathodic polarization of the BOS electrodes and their illumination (Fig. 1a). As is seen, the cathodic current sharply increases under periodic illumination and the IPCE value reaches 550 % at E = –150 mV

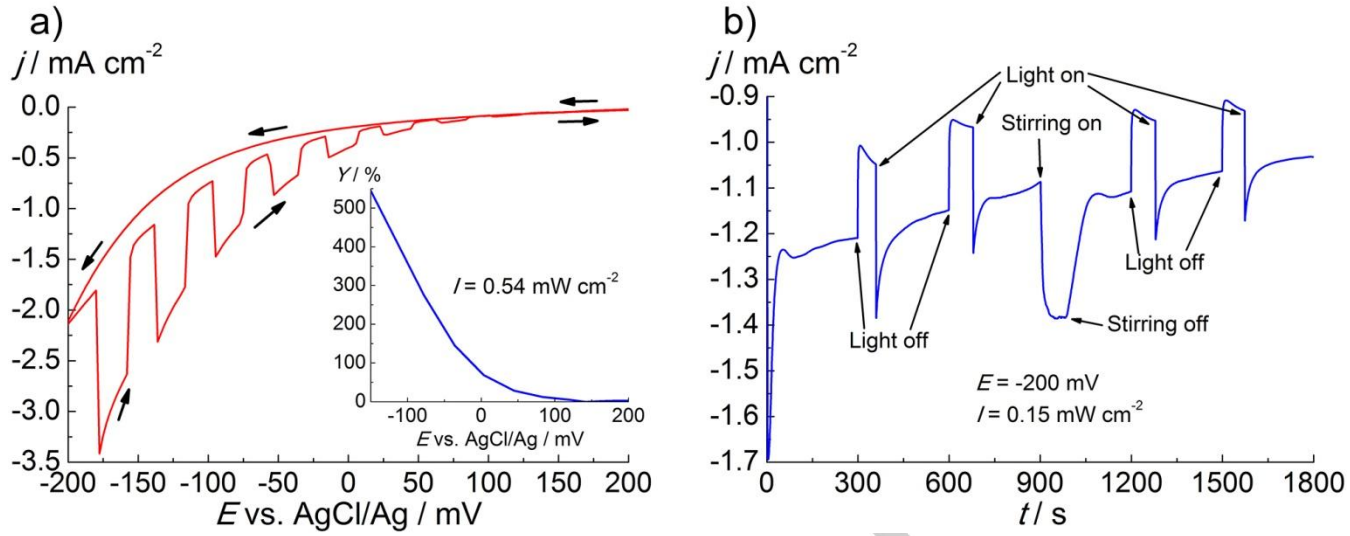

Figure 1. Cyclic voltammograms (CVs) for BOS electrode recorded with a periodic illumination during the anodic scan (a); chronoamperogram at E = –0.2 V (b). The inset in Fig. 1a shows the dependence of IPCE on electrode potential. Solution: 0.05 M $K_3[Fe(CN)_6]$ + 0.05 M $K_4[Fe(CN)_6]$ + 0.1 M K_2SO_4.

in this solution (inset in Fig. 1a). The cathodic current is related to the reaction:

$$[Fe(CN)_6]^{3-} + e^- \rightarrow [Fe(CN)_6]^{4-} \quad (1)$$

The chronoamperogram presented in Fig. 1b demonstrates the strong dependence of the cathodic current on the solution stirring. It points out to the diffusion-limited character of the electrochemical process.

The surface microstructure and phase composition of the BOS electrodes were studied after registration of the chronoamperogram for 30 min corresponding to the passed charge equal to 2 Q cm^{-2}. Fig. 2a presents SEM image of the surface of the pristine electrode. The SEM view of the BOS sample after soaking in the same solution in the open circuit mode in the dark is shown in Fig. 2b. The SEM image of the electrode surface after electrochemical polarization under illumination is given in Fig. 2c. The comparison of these aforementioned images reveals insignificant changes in the surface microstructure with and without electrochemical polarization. It should be also noted that the phase and elemental composition of the film do not change under the electrochemical polarization, electrode lighting and a contact with the solution. This is confirmed by X-Ray Diffraction (XRD) results (Fig. 3), as well as Energy-Dispersive X-ray (EDX) analysis (Table S1). The optical transmission of BOS films after the same treatment is also practically unchanged (Fig. S1).

It is known that the photoelectrochemical oxidation of semiconductors is related to the reactions involving valence band photoholes, whereas the photoreduction reactions proceed with the participation of conduction band electrons [18,19]. The decomposition of a semiconductor takes place if the potentials of its reductive and oxidative decomposition belong to the range of electrode potentials between the valence band top and conduction band bottom [18].

Under illumination, the photoelectrons are excited from valence to conduction band. It leads to the weakening of the chemical bonds between the atoms of semiconductor and facilitation of the photocharges interaction with electrolyte species [20].

The disappearance of giant IPCE effect in $[Fe(CN)_6]^{3-}$/$[Fe(CN)_6]^{4-}$ takes place under the BOS electrode cathodic polarization at the potentials E < –0.8 V.

More negative polarization of the film can result in the reduction of bismuth ions of the BOS lattice:

$$Bi^{3+} + 3e^- \rightarrow Bi^0 \quad (2)$$

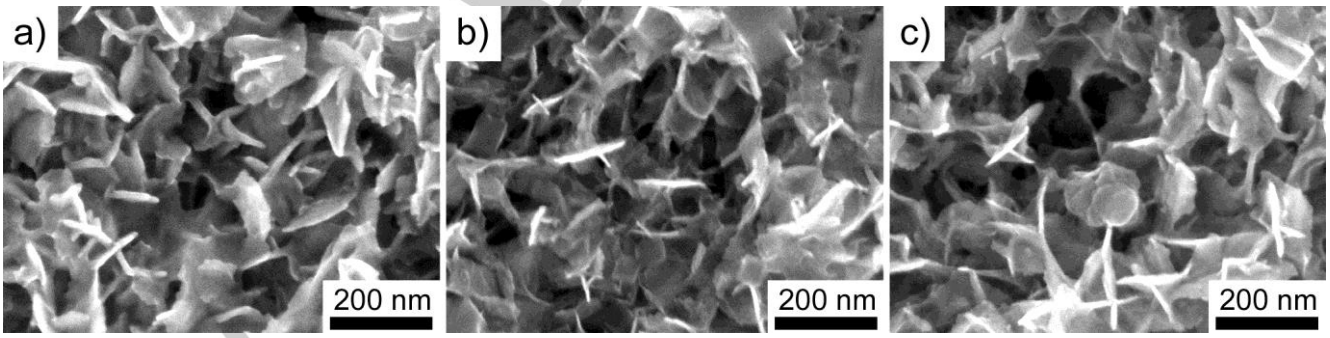

Figure. 2. SEM images of BOS film before (a) and after (b) dipping in 0.05 M $K_3[Fe(CN)_6]$ + 0.05 M $K_4[Fe(CN)_6]$ + 0.1 M K_2SO_4 solution for 1 h in the open circuit mode, as well as after polarization at E = –200 mV for 0.5 h (c)

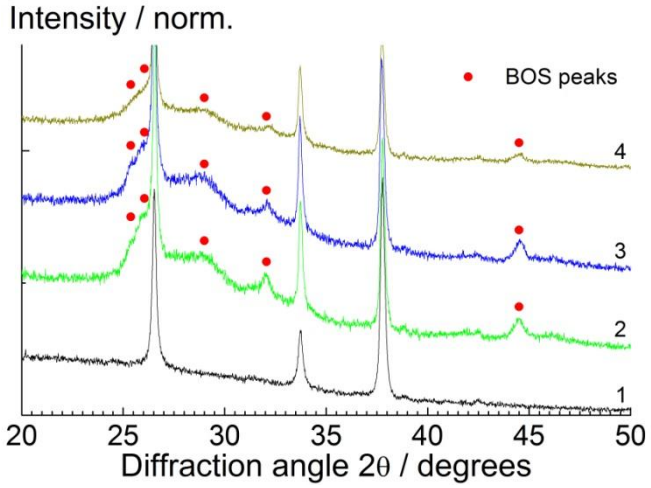

Figure. 3. XRD patterns of FTO (curve 1) and BOS films before (curve 2) and after (curve 3) contact with the 0.05 M $K_3[Fe(CN)_6]$ + 0.05 M $K_4[Fe(CN)_6]$ + 0.1 M K_2SO_4 electrolyte without polarization for 1 h, as well as after polarization for 0.5 h at *E* = –200 mV (curve 4).

Taking into account the values of the standard reduction potential E^0 for bismuth oxide and sulfide [21,22]:

$$Bi_2O_3 + 6H^+ + 6e^- \rightarrow Bi^0 + 3H_2O \qquad E^0 = -0.46 \text{ V (pH 7)} \qquad (3)$$

$$Bi_2S_3 + 6e^- \rightarrow Bi^0 + 3S^{2-} \qquad E^0 = -0.84 \text{ V (pH 7)} \qquad (4)$$

we can presume that E^0 lies in the range from –0.46 to –0.84 V for bismuth oxysulfide. To avoid the films destruction, we did not polarize them in the range of potentials $E < -0.8$ V which corresponds to the bismuth oxysulfide reduction.

While the chemical instability of the BOS in reduction processes is related to reaction (2), its lability to oxidizing agents can be connected with the oxidation of the lattice sulfide anions. As the giant IPCE effect is observed under cathodic polarization of electrode, there is no oxidation by photoholes. Thus, photooxidative processes do not play any significant role in the implementation of the giant IPCE effect.

As was noted above, the chemical composition change of the surface of semiconductors could be a result of surface chemical reactions of the semiconductor with electrolyte components. We have found that with a long-term presence of a BOS film in a ferrocyanide solution for 3 and 7 days, an increase in the optical transmission of the films is observed (Fig. S2). Such "enlightenment" reaches 20–30% illustrating the chemical instability of the BOS film in this electrolyte. At the same time, XRD demonstrates retention of the phase composition (Fig. S3) indicating a gradual decrease of the film thickness as the most plausible reason of the observed transmission increase.

The formation of slightly soluble compound phase can be visible when the film comes in a contact with concentrated 0.5 M of $K_3[Fe(CN)_6]$ aqueous solution. At the same time, the BOS film microstructure and elemental composition (Table S1) does not significantly change by exception of appearance of large well-grained crystals evenly scattered on the surface (Fig. 4a).

Accordingly there are narrow reflexes associated with these crystals on XRD pattern (Fig. 4b). The lines could be attributed to $K[BiFe(CN)_6]\cdot 3H_2O$ phase of a hexagonal syngony with unit cell parameters *a* = 0.1345 nm, *c* = 1.3445 nm [23,24]. The formation of $K[BiFe(CN)_6]$ crystallites on BOS electrode surface in contact with $[Fe(CN)_6]^{4-}$ anions of electrolyte can be expressed as a result of the chemical interaction:

$$Bi^{3+} + [Fe(CN)_6]^{3-} \rightarrow [BiFe(CN)_6]^- \qquad (5)$$

by analogy with a well-known analytical reaction of the "Prussian Blue" formation:

$$Fe^{3+} + [Fe(CN)_6]^{3-} \rightarrow [FeFe(CN)_6]^- \qquad (6)$$

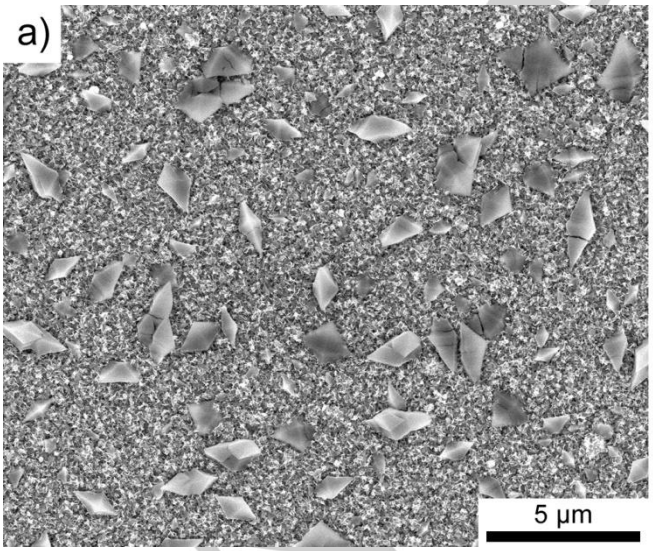

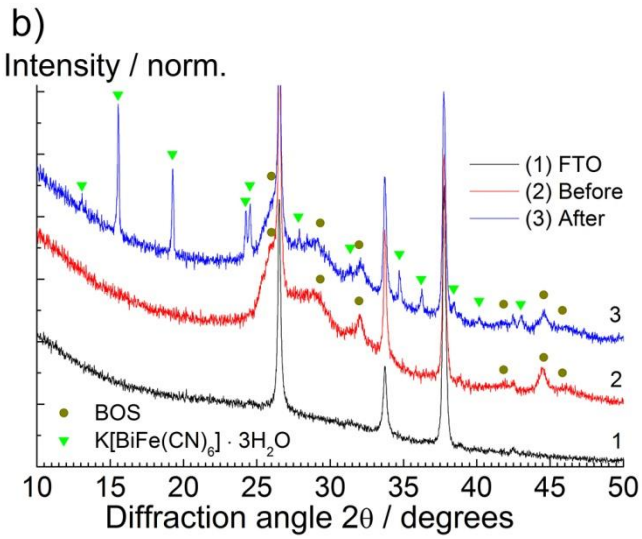

Figure. 4. SEM image of the BOS film after electrochemical polarization in 0.5 M $K_3[Fe(CN)_6]$ at *E* = -200 mV during 30 min (a), XRD patterns of FTO (1), initial BOS film (2) and BOS film after electrochemical polarization in 0.5 M $K_3[Fe(CN)_6]$ at *E* = -200 (b).

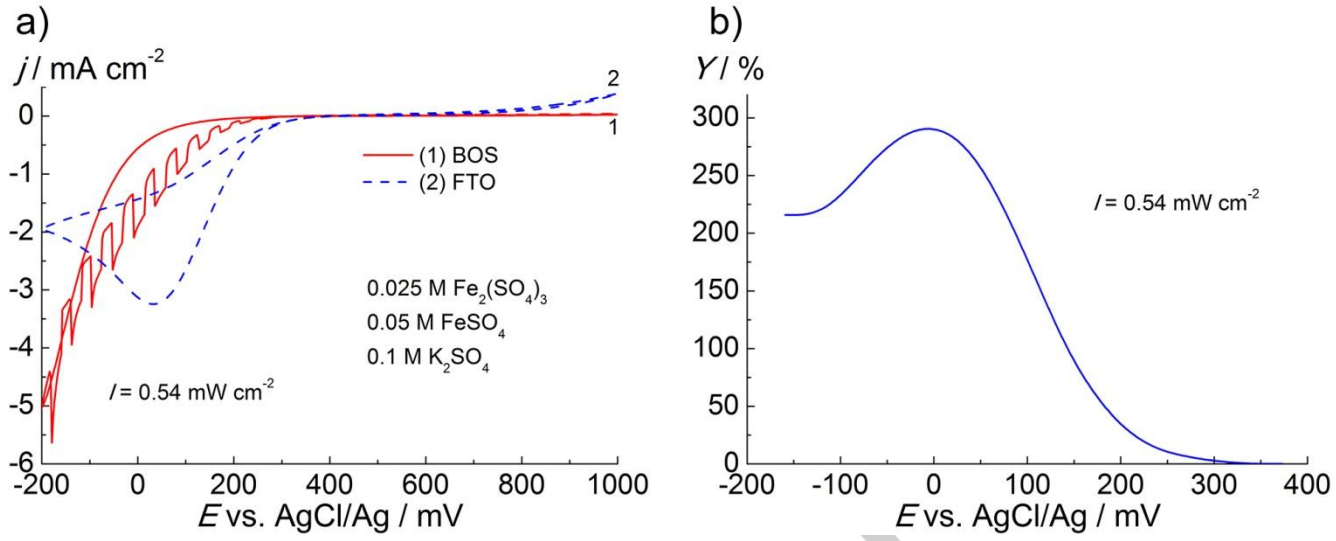

Figure 5. Cyclic voltammograms for BOS (1) and reference FTO electrode (2) in Fe^{3+}/Fe^{2+} redox system (a); dependence of IPCE on electrode potential derived from the voltammogram (b).

The rate of the formation of a poorly soluble deposit accordingly the reaction (5) depends on the concentration of $[Fe(CN)_6]^{4-}$ and Bi^{3+} ions. During the cathodic process the concentration of $K_4[Fe(CN)_6]$ in the near-electrode area increases not only due to the reduction of $[Fe(CN)_6]^{3-}$ (Eq. 1) but also by chemical oxidation of S^{2-} ions in BOS lattice by $[Fe(CN)_6]^{3-}$ anions. The oxidation of surface S^{2-} anions can also contribute to an increase in the rate of transition of Bi^{3+} ions into the ferrocyanide complex. The gradual chemical transformation of BOS into a poorly soluble bismuth ferrocyanide $K[BiFe(CN)_6]\cdot 3H_2O$ ultimately leads to the destruction of the BOS film. In particular in 0.5 M $K_3[Fe(CN)_6]$ electrolyte a complete destruction of 670 nm thick BOS film occurred in 70–80 hours.

BOS electrodes in Fe^{3+}/Fe^{2+} containing solution

The giant IPCE effect is also observed in $Fe_2(SO_4)_3$ / $FeSO_4$ aqueous solution (Fig. 5a), and the dependence of IPCE on the electrode potential has a maximum at E = 0.0 V. This is related to the instability of the BOS films in 0.025 M $Fe_2(SO_4)_3$ + 0.05 M $FeSO_4$ + 0.1 M K_2SO_4 solution which leads to their gradual dissolution. The origin of this instability is connected with the hydration of Fe^{3+} cations with formation of aqua complexes being the strong Brönsted acids:

$$[Fe(H_2O)_6]^{3+} + H_2O \leftrightarrow [Fe(H_2O)_5OH]^{2+} + H_3O^+ \quad (5)$$

As a result of hydrolysis reactions, the used aqueous solution of iron sulfates was acidic with pH 2.5. In such conditions, the BOS film gradually dissolves, and its thickness decreases. As it was demonstrated earlier, the IPCE value depends on a number of factors including film thickness [12]. The change of the film thickness during the cathodic polarization curve record could be responsible for the appearance of the maximum at IPCE–E dependence (Fig. 5b). Such high reactivity of the BOS films in acidic solutions can be connected with thin platelet-like crystals possessing high concentration of defects [12].

Thus, along with the aforementioned corrosion instability of the BOS films related to redox reactions, another aspect of chemical instability is related to photolytic reactions in acidic solutions.

BOS electrodes in I_2^-/I^- containing solution

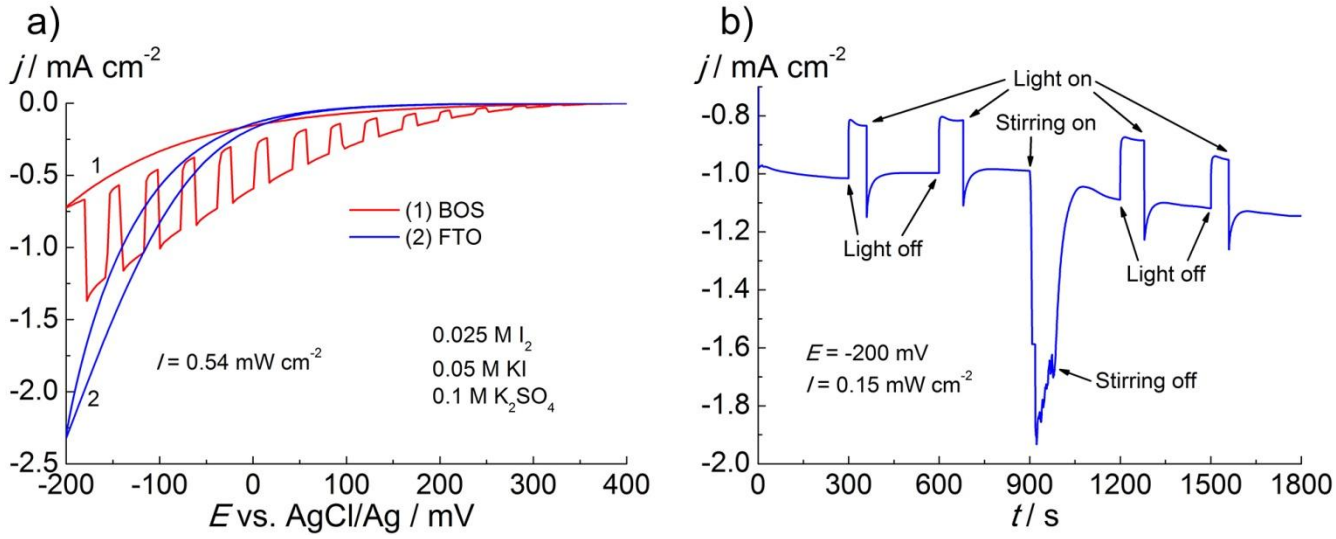

Figure 6. Cyclic voltammograms for BOS (1) and reference FTO electrode (2) in the iodine-iodide redox system (a) and chronoamperogram (b) of BOS electrode in the same solution.

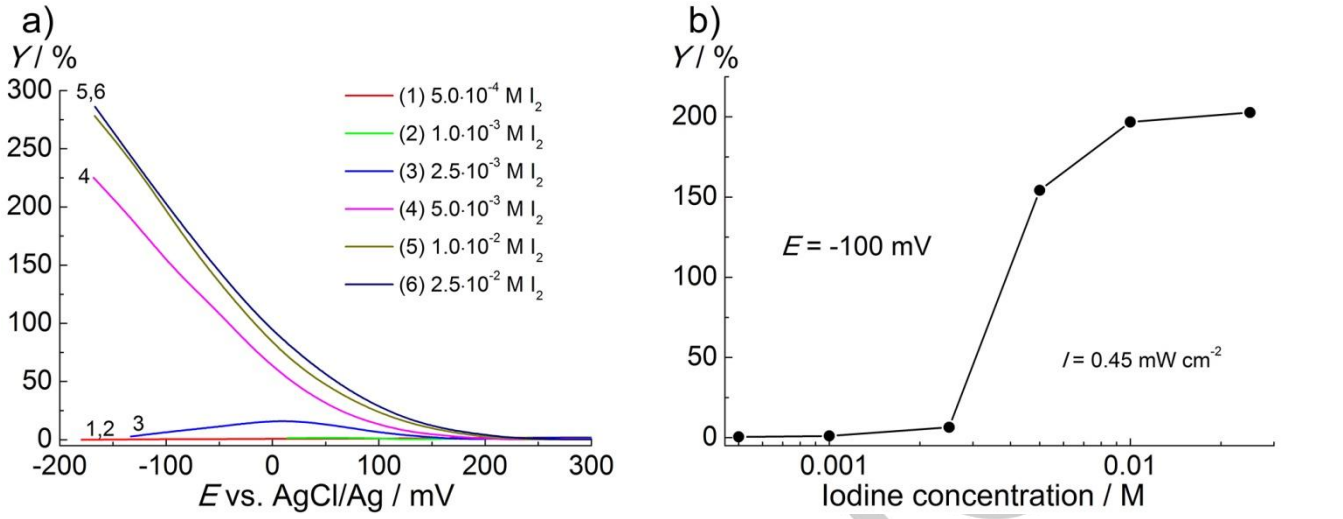

Figure 7. Dependence of IPCE for BOS electrode on the electrode potential (a) and concentration of the molecular iodine (b).

The giant IPCE effect is clearly manifested in aqueous solutions containing I_2^-/I^- redox system (Fig. 6). The photocurrent appears at $E < +0.2$ V existing along with the comparable dark current (Fig. 6a, curve 1). The cathodic dark and photoinduced processes are related to the reduction of molecular iodine:

$$I_2 + 2e \rightarrow 2I^- \quad (6)$$

The diffusion-limited type of the cathodic process is well illustrated by the chronoamperogram obtained at $E = -0.2$ V (Fig. 6b). The solution stirring results in the growth of the dark and the photocurrent. After stop of the stirring, the cathodic current rapidly relaxes to the initial value confirming that the Faraday process is limited by I_2 delivery to the electrode surface.

The dependences of IPCE on the electrode potential and I_2 concentration are presented in Fig. 7. The IPCE exceeds 100% at $E < 0$ V and reaches ~300% at $E = -0.2$ V (Fig. 7a). For the oxidizer concentrations $c < 5 \cdot 10^{-3}$ M, the cathodic current is very small or is not detected. At $c > 1 \cdot 10^{-2}$ M, the photocurrent value is not affected by the concentration (Fig. 7b). The presented behavior of IPCE vs. concentration is very similar to the dependence obtained by us earlier for $[Fe(CN)_6]^{3-}$ solutions [11].

SEM study of the BOS electrodes surface after the record of chronoamperogram presented in Fig. 6b indicates the change in the surface morphology (Figs. 8a and 8b). The contact of BOS film with the aqueous solutions containing I^- anions leads to a gradual change in the elemental composition of the film: reduction of the sulfur content and enrichment it with iodine (Table S1). An increase in the concentration of the oxidizing agent (I_2) contributes to an increase in the rate of the exchange process. The XRD analysis revealed that bismuth oxyiodide BiOI is formed on the surface of the BOS electrodes in the I_2/I^- solution (Fig. 8a).

As is known, both bismuth oxyiodide and oxysulfide possess the similar layered structure [25]. The main difference consists in the Van der Waals planes in BiOI formed by the iodine atoms instead the sulfur atoms in bismuth oxysulfide [1–7,9–11,13,14,17]. Under a contact of the BOS with I_2^-/I^- solution, the formation of BiOI takes place due to the ion exchange reaction between S^{2-} anions in semiconductor and I^- anions in solution.

Exchange process on the surface of BOS electrodes in the I_2/I^- containing solution also proceeds in the open circuit mode. It accelerates with the concentration increase of both iodide anions and molecular iodine (Fig. 8a). A full chemical conversion of BOS to BiOI is possible during approximately one week (Fig. 9a, curve 5, Table S1). It is in agreement with the Raman spectroscopy data (Fig. 9b) which demonstrate the appearance of two sharp peaks at 87 and 151 cm^{-1}. They correspond to photon scattering on phonons with A_{1g} and E_g symmetry [26–28]. The formation of BOS/BiOI heterostructure does not block the cathodic dark and photocurrent. This indicates that all the solid-state interfaces do not have any energy barriers disturbing the transport of charge carriers.

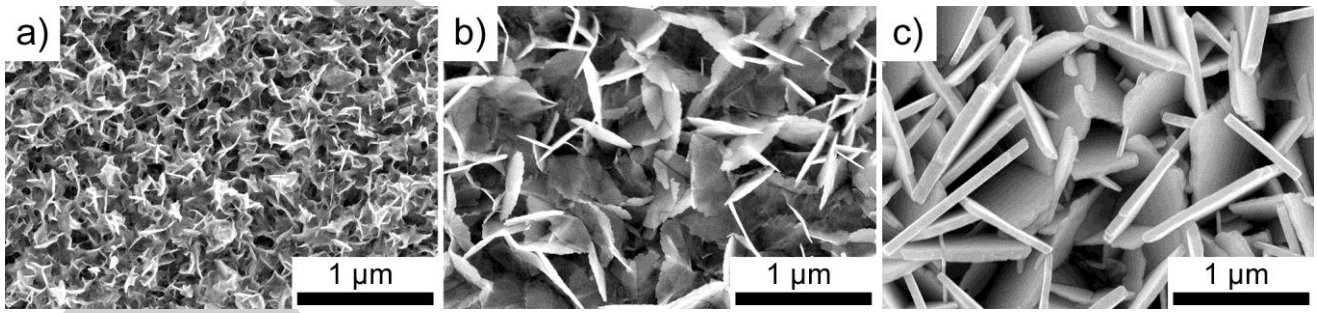

Figure 8. SEM images of BOS film before (a), after (b) polarization for 0.5 h at $E = -200$ mV in 0.025 M I_2 + 0.05 M KI + 0.1 M K_2SO_4 aqueous solution and dipping in solution for 7 days in the open circuit mode (c).

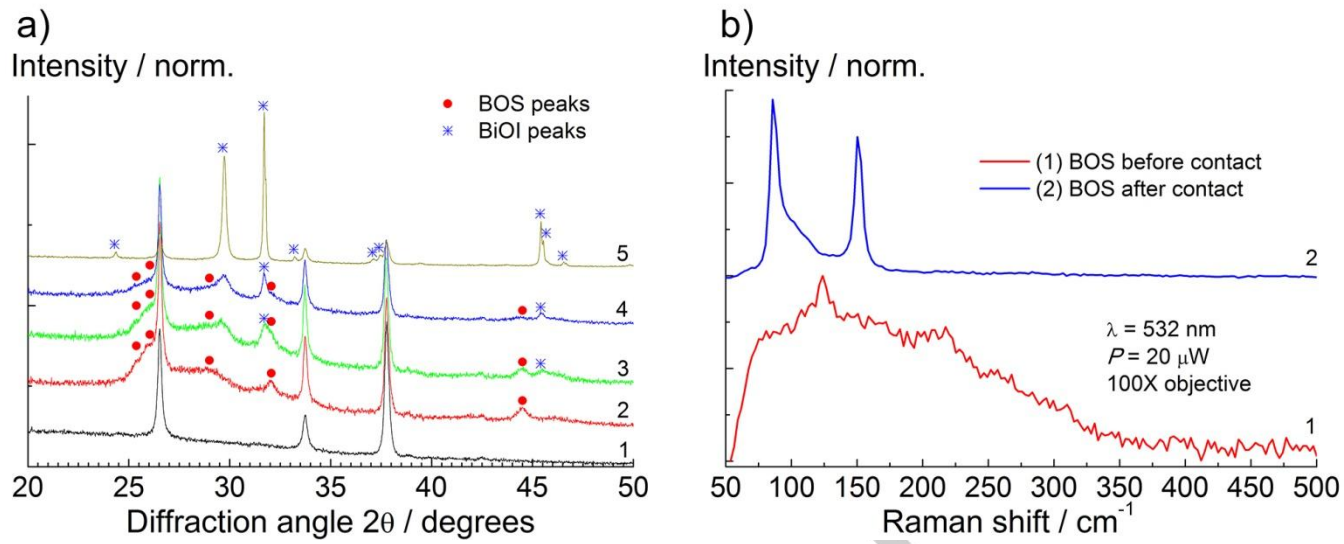

Figure 9. XRD patterns for FTO film (1) and BOS film on FTO: before contact with the electrolyte (2), after soaking without polarization for 1 h in 0.025 M I_2 + 0.05 M KI + 0.1 M K_2SO_4 aqueous solution (3), after polarization for 0.5 h at E = –200 mV in the same solution (4); after soaking without polarization for 7 days in the same solution (5); Raman spectra of BOS film before (1) and after (2) contact with electrolyte for 7 days

BOS electrodes in polysulfide electrolyte

There is no giant IPCE effect in polysulfide (S_n^{2-}/S^{2-}) electrolyte (Fig. 10a) due to a high electrocatalytic activity of BOS film in the cathodic reduction of S_n^{2-} anions. As is seen from Fig. 10a, the cathodic polarization of the BOS electrode is accompanied by a sharp increase of current at $E <$ –0.7 V. Therefore, the illumination does not influence on the rate of the cathodic reaction. The reference CV curve for FTO substrate demonstrates the absence of electrocatalytic properties. Under the anodic polarization and illumination, the anodic photocurrent with quantum efficiency about 20% is observed.

As we pointed out earlier [11], the anodic photocurrent was revealed also in solutions containing $[Fe(CN)_6]^{3-}/[Fe(CN)_6]^{4-}$ and I_2/I^- redox systems. XRD studies demonstrate that the prolonged (for tens of hours) contact with the polysulfide electrolyte leads to the formation of the bismuth sulfide Bi_2S_3 phase (Fig. 9b). The origin of Bi_2S_3 formation, like in the case of BiOI, is related to the ion exchange reaction: replacement of oxygen in the lattice by sulfur. According to EDX data, this process is accompanied by a sharp increase in the sulfur content (Table S1). At the same time, there is a slight (about 5%) decrease in the transmission of the films (Fig.S4). Since the formation of Bi_2S_3 phase is connected with the diffusion of S^{2-} ions through the BOS film, this process takes a long time. In the case of significantly shorter soaking times (minutes), both XRD and Raman spectra do not demonstrate the formation of Bi_2S_3 phase. Nevertheless, one can expect that formation of S-terminated surface could take place under these conditions due to both ion exchange in thin near-surface layers and chemical absorption of S^{2-} anions [29,30,31].

Electrocatalytic properties of BOS electrode with S-terminated surface

Electrocatalytical activity of the electrodes is mostly determined by the structure of the double electrical layer (DEL). Such DEL parameters as polarity, density of charge, and capacity are determined by the microstructure of the electrode surface.

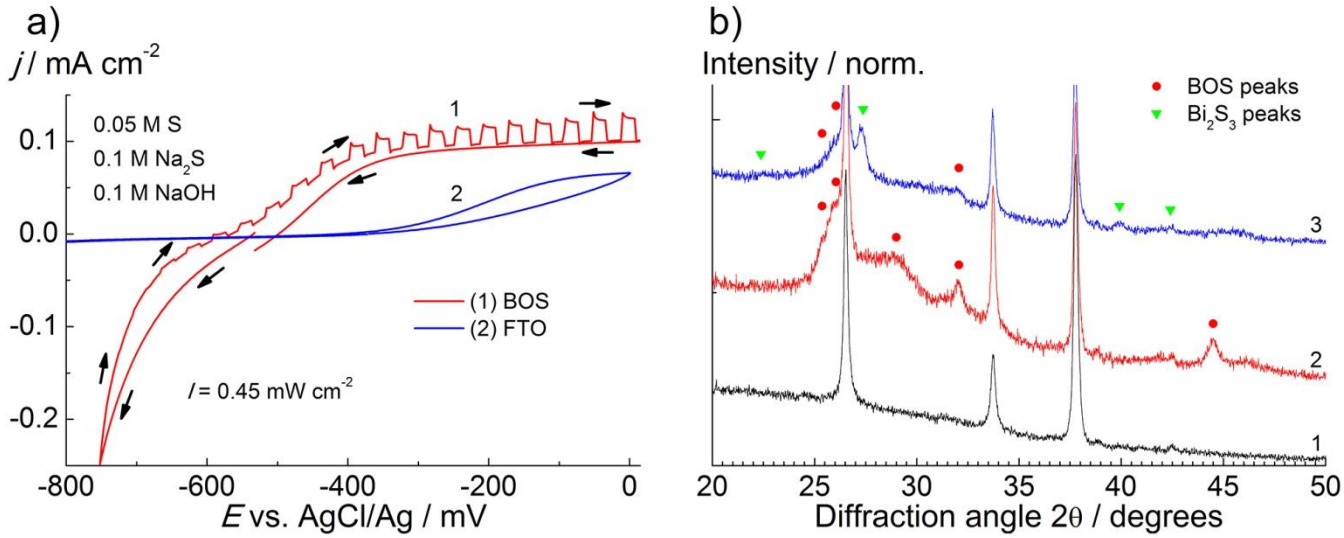

Figure 10. Cyclic voltammograms for BOS (1) and FTO (2) electrodes in polysulfide electrolyte (a); X-ray diffraction patterns of reference FTO (1) and BOS films before (2) and after (3) soaking in 0.05 M Na_2S solution for 8 days (b).

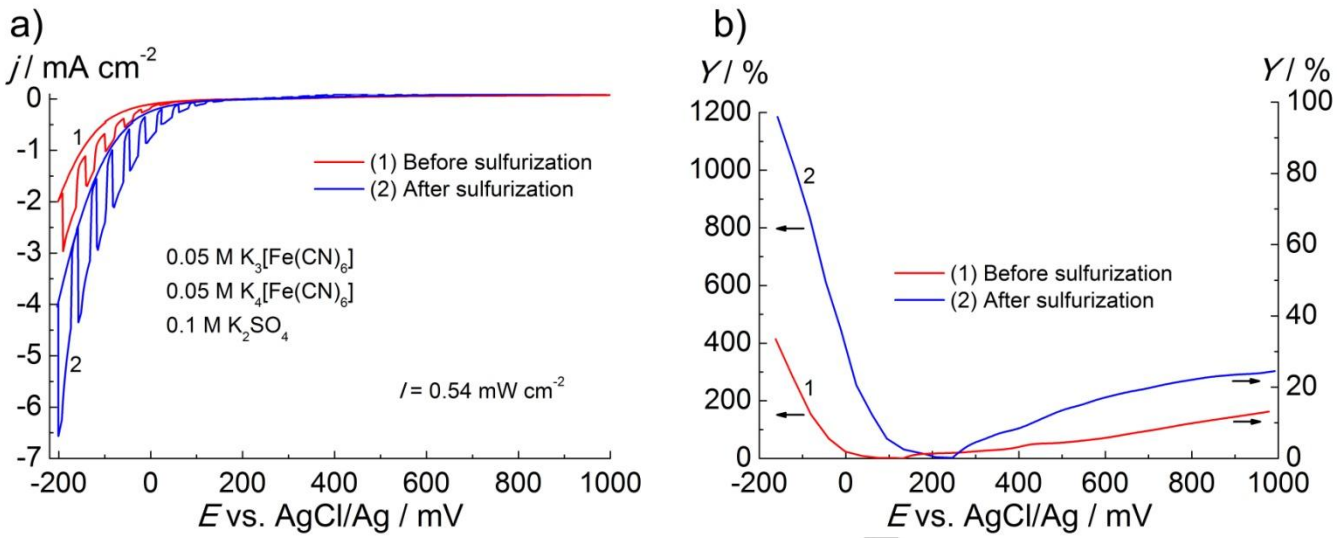

Figure 11. Cyclic voltammograms for BOS electrode before (1) and after (2) treatment in sulfide electrolyte (a); corresponding dependences of IPCE (b).

The presence of the oxygen surface atoms in oxides, e.g. bismuth oxysulfide, promotes the photolytic reactions. The protonation of surface oxygen atoms sufficiently influences on the charge distribution on the interface between the BOS electrode and electrolyte. The enrichment of the bismuth oxysulfide by the sulfur atoms (surface S-termination) leads to the DEL microstructure alteration. As a result, the rate of charge transfer to the heterointerface is changing, and the electrocatalytical properties are also changing respectively.

We revealed that formation of S-terminated surface leads to the significant enhancement of the giant IPCE effect in $[Fe(CN)_6]^{3-}$ /$[Fe(CN)_6]^{4-}$ containing solution. As is seen from Fig. 11a, both dark and especially photocurrent sharply increase after sulfurization. Figure 11b demonstrates that IPCE value increases from 2 to 10 times depending on the electrode potential. This process is related to the photoelectrochemical process on the surface of the BOS films being multistage [12]. It includes such subsequent stages as photogeneration of charge carriers, transfer of electrons in the BOS film, electrochemical discharge, delivery and removal of reagents and reaction products from the surface, *etc*.

The enrichment of the BOS surface by sulfur atoms increases the rate of the cathodic reduction of $[Fe(CN)_6]^{3-}$ and, correspondingly, allows one to control the IPCE value.

Conclusions

The corrosion and photocorrosion stability of BOS films in aqueous solutions is determined by ion exchange, redox, and protolytic processes. In aqueous solutions containing different redox systems ($[Fe(CN)_6]^{3-}$/$[Fe(CN)_6]^{4-}$, I_2/I^-, S_n^{2-}/S^{2-}) the chemical stability of BOS films is mostly related to ion exchange reactions and formation of new weakly soluble compounds such as $K[BiFe(CN)_6]\cdot 3H_2O$, BiOI and Bi_2S_3 in the case of presence of $[Fe(CN)_6]^{4-}$, I^- or S^{2-} ions in the solution. At initial stages of the formation, all mentioned slightly soluble compounds do not prevent the giant IPCE effect.

Since the giant IPCE effect is observed for the cathodic process (1), the stability of the BOS film is maintained while the electrode potential does not reach the cathodic destruction potential of bismuth oxysulfide. The latter process is associated with the reduction of the BOS lattice bismuth ions to metal (2).

The Faraday process related to the giant IPCE effect proceeds in the diffusion-limited mode and for this reason the photocurrent increases with the concentration of electron acceptor. At the same time, the increase of oxidizer concentration promotes the BOS film degradation, accelerating the chemical oxidation of S^{2-} ions of the BOS lattice.

Chemical instability of the BOS films in aqueous solutions is also determined by the protolytic reactions, resulting in destruction of the semiconductor. It has been demonstrated that dissolution of BOS films occurs in acidic solutions at pH < 3. This fact restricts the area of the BOS films application in acidic aqueous solutions. How to enhance the chemical stability of the BOS films? One of the possible ways is the application of non-aqueous media, as well as the usage for aqueous redox systems which do not enter into chemical interaction with BOS. Another way, apparently, consists in coverage of the BOS surface with stable and electrocatalytically active films (metals, oxides, etc.). For example, the deposition of thin films of such a stable oxide as TiO_2 made it possible to significantly increase the corrosion stability of Cu_2O in the reaction of the release of molecular hydrogen [32]. Evaluation of the prospects of these approaches is the subject of independent research, beyond the scope of this work.

Finally, the enrichment of BOS surface with S atoms (S-termination of surface) results in a sharp increase of the elecrocatalytic activity of the BOS film in $[Fe(CN)_6]^{3-}$ cathodic reduction. This leads to up to order increase of IPCE.

Experimental Section

BOS films preparation method

Bismuth oxysulfide films with a thickness of 670 ± 20 nm were grown on fluorine doped tin oxide glass (FTO) substrates using CBD method at 100 °C. The aqueous solutions for CBD contained 0.021 M $Bi(NO_3)_3$, 0.73 M triethanolamine, 0.21 M thiourea and 0.16 M NH_3. The BOS films deposition time comprised 80 min. The CBD technique, kinetics of films growth, their physical and chemical characterization were described in more details in our previous works [11,12].

Equipment and measurement conditions

X-ray diffraction (XRD) measurements were performed with an Empyrean diffractometer (PANalytical, Netherlands) equipped with Cu Kα X-Ray tube and Ni-filter with 0.01 degree step.

Scanning electron microscopy investigations were carried out using a S-4800 scanning electron microscope (Hitachi, Japan). The Energy Dispersion X-Ray (EDX) spectra were collected with an Aztec Energy Advanced X-Max 80 X-ray analyzer (Oxford instruments, United Kingdom).

Transmission spectra were recorded using a MC122 spectrometer (Proscan Special Instruments, Belarus) with a 3 nm slit bandwidth.

Raman spectra were recorded using a Nanofinder HE confocal spectrometer (Lotis TII, Belarus–Japan) with 532 nm solid-state laser as an excitation source. The incident optical power was attenuated down to 20 μW for minimization of thermal impact. The backscattered light without analysis of its polarization was dispersed by a 600 lines mm^{-1} diffraction grating providing spectral resolution better than 2.5 cm^{-1} and registered with a cooled charge coupled device. The signal acquisition time was equal to 60 s. The spectrum calibration was done using a built-in gas-discharge lamp providing the accuracy better than 2.5 cm^{-1}.

Photoelectrochemical measurements were conducted employing an Autolab PGSTAT101 potentiostat in a three electrode electrochemical cell with platinum counter electrode and saturated silver chloride electrode (+0.201 V vs. SHE) as a reference. The reference electrode was separated from the cell with the salt bridge filled with 0.5 M Na_2SO_4 solution. The cyclic voltammogramms were recorded starting from the immersion potential towards the cathodic potential sweep with the chopped illumination during reverse anodic scan. The scan rate was 20 mV s^{-1}. The samples were illuminated from the glass side to prevent the absorption of light by the colored solution. The monochromatic light 465 nm was used in CV measurements. The irradiation of the BOS films during the chronoamperograms record was performed using a 465 nm blue LED.

Acknowledgements

The authors acknowledge N. Brezhneva, L. Ivashkevich, S. Gusakova, as well as employees of the scientific-technical center "Belmicrosystems" of JSC "Integral" for consultations, XRD and SEM investigations.

This work was supported by the State Research Program “Photonics, Opto-, and Microelectronics” of the Republic of Belarus (task 1.2.02).

Keywords: bismuth oxysulfides, giant IPCE, photoelectrochemistry of semiconductors, corrosion stability, S-terminated surface

[1] E. Koyama, I. Nakai, K. Nagashima, *Acta Crystallogr.* 1984, 40, 105-109.

[2] L. Pacquette, H. Hagiwara, T. Ishihara, A. A. Gewirth, *J. Photochem. Photobiol.* A 2014, 277, 27-36.

[3] X. Zhang, Y. Liu, G. Zhang, Y. Wang, H. Zhang, F. Huang, *ACS Appl. Mater. Interfaces* 2015, 7, 4442-4448.

[4] W. A. Phelan, D. C. Wallace, K. E. Arpino, J. R. Neilson, K. J. Livi, C. R. Seabourne, T. M. McQueen, *J. Am. Chem. Soc.* 2013, 135, 5372-5374.

[5] J. Shao, Z. Liu, X. Yao, L. Pi, S. Tan, C. Zhang, Y. Zhang, *Phys. Status Solidi Rapid Res. Lett.* 2014, 8, 845-848.

[6] L. Li, D. Parker, P. Babkevich, L. Yang, H. M. Ronnow, A. S. Sefat, *Phys. Rev. B* 2015 91, 104511.

[7] Y. Mizuguchi, H. Fujihisa, Y. Gotoh, K. Suzuki, H. Usui, K. Kuroki, S. Demura, Y. Takano, H. Izawa, O. Miura, *Phys. Rev. B* 2012, 86, 220510(R).

[8] S. G. Tan, L. J. Li, Y. Liu, P. Tong, B. C. Zhao, W. J. Lu, Y. P. Sun, *Physica C Supercond.* 2012, 483, 94-96.

[9] G. Liu, D. Li, S. Li, J. Wang, Z. Zhang, *Physica C* 2015, 510, 27-30.

[10] S. Meng, X. Zhang, G. Zhang, Y. Wang, H. Zhang, F. Huang, *Inorg. Chem.* 2015, 54, 5768-5773.

[11] E. A. Bondarenko, E. A. Streltsov, M. V. Malashchonak, A. V. Mazanik, A. I. Kulak, E. V. Skorb, *Adv. Mater.* 2017, 29, 1702387.

[12] E. A. Bondarenko, E. A. Streltsov, A. V. Mazanik, A. I. Kulak, V. Grivickas, P. Scajev, E. V. Skorb, *Phys. Chem. Chem. Phys.* 2018, 20, 20340-20346.

[13] A. Miura, Y. Mizuguchi, T. Takei, N. Kumada, E. Magome, C. Moriyoshi, Y. Kuroiwa, K. Tadanaga, *Solid State Commun.* 2016, 227, 19-22.

[14] H. Kotegawa, Y. Tomita, H. Tou, H. Izawa, Y. Mizuguchi, O. Miura, S. Demura, K. Deguchi, Y. Takano, *J. Phys. Soc. Jpn.* 2012, 81, 103702.

[15] S. K. Singh, A. Kumar, B. Gahtori, G. Sharma, S. Patnaik, V. P. Awana, *J. Am. Chem. Soc.* 2012, 134, 16504-16507.

[16] G. C. Kim, M. Cheon, D. Ahmad, Y. S. Kwon, R. K. Ko, Y. C. Kim, *J. Phys. Soc. Jpn.* 2018, 87, 025003.

[17] C. Sathish, H. L. Feng, Y. Shi, K. Yamaura, *J. Phys. Soc. Jpn.* 2013, 82, 074703.

[18] H. Gerischer, *Faraday Discuss. Chem. Soc.* 1980, 70, 137-151.

[19] H. Gerischer, *J. Electroanal. Chem. Interfacial Electrochem.* 1977, 82, 133-143.

[20] H. Gerischer, W. Mindt, *Electrochim. Acta* 1968, 13, 1329-1341.

[21] D. R. Lide in *Handbook of Chemistry and Physics*, 84th Ed., CRC press, 2004 pp. 1218

[22] L. M. Peter, *J. Electroanal. Chem. Interfacial Electrochem.* 1979, 98, 49-58.

[23] R. S. Saxena, C. S. Bhatnagar, *Fresenius J. Anal. Chem.* 1959, 165, 95-99.

[24] V. S. Perera, J. Hao, M. Gao, M. Gough, P. Y. Zavalij, C. Flask, J. P. Basilion, S. D. Huang, *Inorg. Chem.* 2011, 50, 7910-7912.

[25] J. Li, Y. Yu, L. Zhang, *Nanoscale* 2014, 6, 8473-8488.

[26] J. E D. Davies, *J. Inorg. Nucl. Chem.* 1973, 35, 1531-1534.

[27] J. Cao, B. Xu, H. Lin, B. Luo, S. Chen, *Dalton Trans.* 2012, 42, 11482-11490.

[28] M. E. Kazyrevich, M. V. Malashchonak, A. V. Mazanik, E. A. Streltsov, A. I. Kulak, C. Bhattacharya, *Electrochim. Acta* 2016, 190, 612-619.

[29] T. V. Lvova, M. S. Dunaevskii, M. V. Lebedev, A. L. Shakhmin, I. V. Sedova, S. V. Ivanov, *Semiconductors* 2013, 47, 721-727.

[30] T. V. Lvova, A. L. Shakhmin, I. V. Sedova, M. V. Lebedev, *Appl. Surf. Sci.* 2014, 311, 300-307.

[31] M. V. Lebedev, E. V. Kunitsyna, W. Calvet, T. Mayer, W. Jaegermann, *J. Phys. Chem. C* 2013, 117, 15996-16004.

[32] J. Luo, L. Steier, M.-K. Son, M. Schreier, M. T. Mayer, M. Grätzel, *Nano Lett.* 2016, 16, 1848–1857.

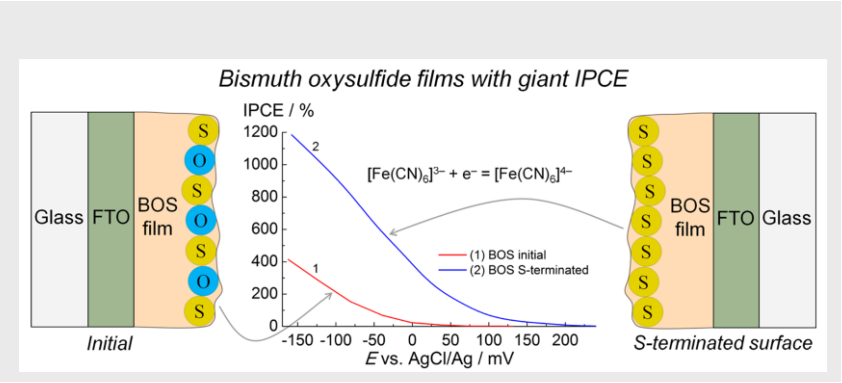

Evgeny A. Bondarenko, Eugene A. Streltsov, Alexander V. Mazanik, Anatoly I. Kulak*

Page No. – Page No.

Bismuth oxysulfide photoelectrodes with giant incident photon-to-current conversion efficiency: chemical stability in aqueous solutions

The scheme illustrates the formation of S-terminated surface on the bismuth oxysulfide film and great increase of IPCE in $[Fe(CN)_6]^{3-}$ reduction reaction.